Proceedings of the ASME 2023
International Mechanical Engineering Congress and Exposition
IMECE2023
August 20-23, 2023, Boston, Massachusetts

IDETC2023-117114

MULTI-INPUT MULTI-OUTPUT VIBRATION MODEL FOR MOTORBIKE EXCITED BY RIDE TEST

Massimo Cavacece[1,†,*], Giorgio Figliolini[1,†], Chiara Lanni [1, *]

[1]Department of Civil and Mechanical Engineering, University of Cassino and Southern Lazio, Frosinone, Italy

ABSTRACT

This research proposes a multi–input multi–output model (`MIMO`) to identify the modal properties of a motorbike during the riding test. The MIMO process verifies that a linear combination of all inputs causes each output, and there are no causal relationships between the inputs. If there are causal relationships between one of the outputs, the MIMO process redefines the input signals. The process verifies the connection between input-output and the presence of noise extraneous to the inputs and outputs. The MIMO process represents a multiple-input system with a single output. The peculiar aspect is the decoupling of individual information. In the presence of coupling between the separate inputs, the authors propose the principal component analysis (PCA) to decouple the inputs.

Keywords: Multi-input Multi-output, Modal properties, Comfort Assessment, Ride Test

NOMENCLATURE

ϕ_i	phase offset [rad]
L	road irregularity lenght [Hz]
v	motorbike speed [ms^{-1}]
t	time [s]
$x_1(t)$, $x_2(t)$	input [m]
$x_3(t)$	output [m]
$x_{1\cdot 12,(i-1)}(t)$	conditioned input record [m]
$S_{ij}(f)$	cross-spectral density function [dB]
$\boldsymbol{M}$	mass matrix
$\boldsymbol{C}$	damping matrix
$\boldsymbol{K}$	stiffness matrix
$\boldsymbol{G}$	impedance matrix
$\boldsymbol{H}$	frequency response matrix
m_{ij}	virtual signal
$\boldsymbol{S}$	Hermitian matrix
$\boldsymbol{Z}_i$	fictitious process
$p_{i,n}$	poles
Q_r	residue
$z_{i,n}$	zeros
PCA	principal component analysis

[†]Joint first authors
[*]Corresponding author: cavacece@unicas.it
Documentation for `asmeconf.cls`: Version 1.34, December 13, 2023.

1. INTRODUCTION

Motorbike manufacturers analyze the vibrations on the driver and passengers inside the motorbike generated by the rough road surface. Motorike testing procedures are defined by the international ISO standard. The researchers consider mechanical models equivalent to concentrated parameters offering a quantitative assessment of motorbike accelerations in terms of natural frequencies and motorbike dissipative properties [1]. A combination of masses, stiffness, and damping parameters represents the motorbike components. The lumped parameter models and the finite element method use models for distributing these parameters to form complete matrices of mass, stiffness, and damping for each component. If research considers large complex systems, better computing may require simplifying the mechanical model. Suppose the mathematical model analyzes the vibrations of a motorbike due to excitation of the unidirectional terrain. In that case, the simplified approach considers the molded car tires as a spring-damper system, ignoring the non-linear behavior of the tires [2]. The noise of the engine, the road, and the dynamic action induced by the wind, are inputs that generate the mechanical vibrations acquired in the different parts of the interior of a machine, such as mechanical system outputs. The experimental modal analysis uses several agitators to excite the mechanical structure according to the three axes and simultaneously acquires a large number of response signals. Single-input single-output (SISO) estimation methods or simplified mathematical models should not be used in such cases [3]. Comprehensive research on motorbike dynamics should consider the autospectrum between each input and all other signals (including other input signals). This approach allows the analysis of all the mechanical system input/output relations through the frequency response function estimators for MIMO models. The success of frequency response function estimation provides the correct understanding of

the different effects of excitation signals, signal-to-noise ratios, and noise on input or output signals [4]. This research considers the motorbike as a multi-input, multi-output system, where additional inputs in the form of noise on measured signals might affect the behaviour of the motorbike. The Authors consider the motorbike to be linear and time invariant during stationary random processes. The frequency response matrices of multi-input multi-output process include the modal properties of the motorbike. The theorem of partial fraction expansion develops the frequency response matrices in terms of residues and poles of the mechanical system.

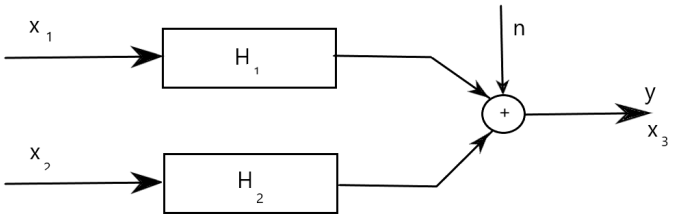

FIGURE 1: TWO-INPUT, SINGLE-OUTPUT SYSTEM, EQN. (??): $z = (r, \phi)$ [3]

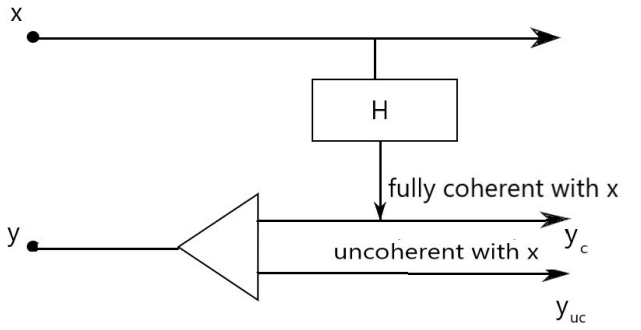

FIGURE 2: COHERENT AND UNCOHERENT SIGNALS, EQN. (??): $z = (r, \phi)$ [3]

2. SPECTRAL FUNCTIONS

The direct approach identifies the output $x_3(t)$ arising from inputs $x_1(t)$ and $x_2(t)$.

The finite Fourier transforms `F.T.` of any pair of data $x(t)$ and $x(t)$ of length T will be defined by the following relations

$$\begin{aligned} X(f) &= x(t)\, e^{-J2\pi f t}\, dt \\ Y(f) &= y(t)\, e^{-J2\pi f t}\, dt \end{aligned} \tag{1}$$

The autospectral density functions $S_{xx}(f)$, $S_{yy}(f)$ and the associated cross–spectral density function $S_{xy}(f)$ associated with transient random processes $x(t)$ and $y(t)$ will be defined by the following relations:

$$\begin{aligned} S_{xx}(f) &= \mathbf{E}\left[|X(f)|^2\right] \\ S_{yy}(f) &= \mathbf{E}\left[|Y(f)|^2\right] \text{ and} \\ S_{xy}(f) &= \mathbf{E}\left[|X^*(f) \cdot Y(f)|^2\right] \end{aligned} \tag{2}$$

where $\mathbf{E}[\ldots]$ indicates the expected value operation. The $S_{xx}(f)$, $S_{yy}(f)$ and $S_{xy}(f)$ relations are two–sided functions with $-\infty < f < \infty$. The symbol * indicates the complex conjugate quantity. The definitions of $S_{xx}(f)$, $S_{yy}(f)$ and $S_{xy}(f)$ relations are appropriate also for stationary random processes.

2.1 Complete Model for Conditioned Inputs

The original input values are $x_i(t)$ with $i = 1, 2, \ldots, n$ and the output signal is $y(t) = x_{i+1}(t)$. Preliminary classification of input signals $x_i(t)$ with $i = 1, 2, \ldots, n$ required as a priori knowledge. Principal Component Analysis (PCA) is a general approach to explore signal correlation patterns $x_i(t)$ with $i = 1, 2, \ldots, n$.

The functions $H_i(f)$ indicate the optimum frequency response functions between each input signals $x_i(t)$ and the output signal $y(t)$. The unknown independent noise term $n(t)$ indicates the deviations between the theoretical linear model (Figure 1) and the experimental investigations.

The complete model indicates $x_{1\cdot 12,(i-1)}(t)$ as the conditioned input records. The term $x_{i\cdot 12,\ldots,(i-1)}(t)$ represents the conditioned input x_i with reffering to the previous input $x_{i-1}(t)$. The PCA removes the linear effects caused by input signals $x_1(t), \ldots, x_{i-1}(t)$ on input signal $x_i(t)$.

If conditioned inputs are q terms, the output $Y = X_{q+1}$ assumes the following relation:

$$Y(f) = X_{q+1}(f) = \sum_{i=1}^{q} H_i(f)\, X_{i\cdot 12,\ldots,(i-1)}(f) + X_{(q+1)\cdot 12,\ldots,q^*} \tag{3}$$

with $X_{(q+1)\cdot 12,\ldots,q^*}(f)$ the noise term $N(f)$.

2.2 Residual Spectra by Gaussian Elimination

If $q = 2$, the mechanical system presents two inputs $x_1(t)$, $x_2(t)$ and one output $x_3(t)$ (Fig.1). The inputs $x_1(t)$, $x_2(t)$ must not be related (Fig.2). An additional contaminating noise $n(t)$ is added to the inputs $x_1(t)$ and $x_2(t)$ to generate the output $x_3(t)$. In the frequency domain, the output of the system is the following relation:

$$\begin{aligned} X_3(f) &= H_1(f)\, X_1(f) + H_2(f)\, X_2(f) + N(f) \\ &= \begin{bmatrix} H_1(f) & H_2(f) \end{bmatrix} \begin{Bmatrix} X_1(f) \\ X_2(f) \end{Bmatrix} + N(f), \end{aligned} \tag{4}$$

The cross–spectral density functions become the following relations

$$\begin{aligned} & S_{11}(f)\, H_1(f) + S_{12}(f)\, H_2(f) = S_{13}(f) \\ & \left(S_{22}(f) - \frac{S_{21}(f)\, S_{12}(f)}{S_{11}(f)}\right) H_2(f) = \\ & S_{33}(f) - \frac{S_{21}(f)\, S_{13}(f)}{S_{11}(f)} \end{aligned} \tag{5}$$

Solving for $H_1(f)$ and $H_2(f)$ using Gaussian elimination

$$H_2(f) = \frac{S_{23\cdot1}(f)}{S_{22\cdot1}(f)} \quad \text{and}$$
$$H_1(f) = \frac{S_{13}(f)}{S_{11}(f)} - \frac{S_{12}(f)\,S_{23\cdot1}(f)}{S_{11}(f)\,S_{22\cdot1}(f)} \tag{6}$$

The residual spectral density function $S_{ij\cdot k}(f)$ can be generalized as

$$S_{ij\cdot k}(f) = S_{ij}(f) - \frac{S_{ij}(f)\,S_{kj}(f)}{S_{kk}(f)} \tag{7}$$

FIGURE 3: FICTITIOUS PROCESSES AND MEASURED SIGNALS, EQN. (??): $z = (r, \phi)$ [3]

2.3 Principal Component Analysis

The cross–spectral density matrix of three processes $x_1(f)$, $x_2(f)$ $x_3(f)$ provides the following matrix

$$\boldsymbol{S}(f) = \begin{bmatrix} S_{11}(f) & S_{12}(f) & S_{13}(f) \\ S_{21}(f) & S_{22}(f) & S_{23}(f) \\ S_{31}(f) & S_{32}(f) & S_{33}(f) \end{bmatrix} \tag{8}$$

The matrix $\boldsymbol{S}$ is Hermitian matrix. The property is that Hermitian matrix $\boldsymbol{S}$ is equal to its conjugate transpose: $\boldsymbol{S} = \boldsymbol{S}^{*T} = \boldsymbol{S}^{H}$.

The determinant and the rank of Hermitian matrix $\boldsymbol{S}$ represent the relationship between the processes $x_i(t)$. The cases are as follows:

- if the processes $x_i(t)$ with $i = 1, 2, 3$ present a linear relationship, the determinant of matrix $\boldsymbol{S}$ is zero and its rank is less than three;
- if the rank of matrix $\boldsymbol{S}$ is 3, there is no linear relationship between the processes $x_i(t)$;
- if the matrix $\boldsymbol{S}$ presents full rank, the Eq.(4) represents the output of the system;
- if the rank the matrix $\boldsymbol{S}$ is less than 3 the method of PCA helps to create new variables m_{11}, m_{12} and m_{13} which are mutually uncorrelated. The new variables m_{ij} generate a matrix $\boldsymbol{M}(f)$. The fictitious processes Z_1, Z_2 and Z_3 describe the measured signals $\boldsymbol{X}(f) = \boldsymbol{M}(f)\,\boldsymbol{Z}(f)$ with

$$\boldsymbol{M}(f) = \begin{bmatrix} m_{11}(f) & m_{12}(f) & m_{13}(f) \\ m_{21}(f) & m_{22}(f) & m_{23}(f) \\ m_{31}(f) & m_{32}(f) & m_{33}(f) \end{bmatrix} \tag{9}$$

The new variables m_{ij} and the fictitious processes Z_i offer the following relations of the measured signals $\boldsymbol{X}(f)$:

$$\begin{Bmatrix} X_1(f) \\ X_2(f) \\ X_3(f) \end{Bmatrix} = \begin{bmatrix} m_{11}(f) & m_{12}(f) & m_{13}(f) \\ m_{21}(f) & m_{22}(f) & m_{23}(f) \\ m_{31}(f) & m_{32}(f) & m_{33}(f) \end{bmatrix} \begin{Bmatrix} Z_1(f) \\ Z_2(f) \\ Z_3(f) \end{Bmatrix} \tag{10}$$

The Eq.(10) underlines that a set of uncorrelated processes $Z_i(f)$ produce the measured signals X_i by the transformation matrix $\boldsymbol{M}$ with $i = 1, 2, 3$ (Fig.3).

3. MODAL IDENTIFICATION BY FREQUENCY RESPONSE FUNCTIONS

Parameter identification estimates unknown parameters in a given dynamical model describing the real system. The proposed method observes the measurable external variables affecting the systems in order to find the value for the missing parameter [5]. The residue Q_r, the zeros $z_{i,n}$ and the poles $p_{i,n}$ of the system are are the unknown parameter vectors. The observations of the in- put and output signals, $x_i(t)$, over the time interval $t_1, t_2, \ldots, t_n$ form the following set of data: $DN = x_1(1), x_2(1), x_3(1), x_1(2), x_2(2), x_3(2), \ldots, x_1(N), x_2(N), x_3(N)$. If $H_i(f)$ are the systems affected by unknown parameters $z_{i,n}$ and $p_{i,n}$ and $N(f)$ denotes the set of non-measurable exogenous signals influencing the systems, an exact mathematical model (and a corresponding simulator) for $H_i(f)$ is available by using experimental investigations. This framework represents the white box identification. The method adopts a suitable function $\bar{f}$ mapping the experimental observations $\bar{f} == x_1(1), x_2(1), x_3(1), x_1(2), x_2(2), x_3(2), \ldots, x_1(N), x_2(N), x_3(N)$. The frequency response matrix $\boldsymbol{H}(s)$ is the inverse of the system impedance matrix $\boldsymbol{G}^{-1}$ in the Laplace domain ($s = \imath\omega = \imath 2\pi f$). The frequency response matrix $\boldsymbol{H}(s)$ of lumped mechanical system assumes the following form:

$$\boldsymbol{H}(s) = \left(s^2 \cdot \boldsymbol{M} + s \cdot \boldsymbol{C} + \boldsymbol{H}\right)^{-1} \tag{11}$$

with $\boldsymbol{M}$ mass matrix, $\boldsymbol{C}$ damping matrix and $\boldsymbol{K}$ stiffness matrix. Therefore, the frequency response matrix $\boldsymbol{H}(s)$ includes the modal properties of the mechanical system. The theorem of partial fraction expansion affirms that any response function $H_i(s)$ is a ratio of two polynomials $P_i(s)$ and $Q_i(s)$:

$$H_i(s) = \frac{Q_i(s)}{P_i(s)} = \frac{(s - z_{i,1})(s - z_{i,2}) \ldots (s - z_{i,n})}{(s - p_{i,1})(s - p_{i,2}) \ldots (s - p_{i,n})} \tag{12}$$

where $z_{i,1}, z_{i,2}, \ldots, z_{i,n}$ are the zeros and $p_{i,1}, p_{i,2}, \ldots, p_{i,n}$ are the poles with $i = 1, 2$ of frequency response matrix $\boldsymbol{H}(s)$.

4. ROAD PROFILE MATHEMATICAL MODELING

The most intensive source of excitation of the motorbike is the road. The factors of the road: length, height, shape, irregularities frequency, and the motorbike speed influences the vertical dynamic behaviour. The irregularities can offer a periodic or random profile of the road. A periodic signal represents the

TABLE 1: STATISTICAL LENGHT AND AMPLITUDE FOR ROAD IRREGULARITY

Road type	h_0 [mm]	L [m]
Motorway-Highway	10–20	10–15
Urban roads (asphalt concrete)	10–20	1.0–2.0
Pavement roads (cobbles)	30–40	0.15–0.30
Offroad	50–70	0.10–0.15

road profile to evaluate the vertical dynamics study. The angular frequency $\omega = 2\pi v$ can be expressed as function of the road irregularity lenght L and motorbike speed v. The Table 1 shows some statistical data. A Fourier series represents the road profile with different frequencies $\omega_1, \omega_2, \ldots, \omega_n$, amplitudes $b_o, b_1, b_2, \ldots, b_n$ of the harmonic components

$$h(t) = b_0 + b_1 \sin(\omega_1 t + \phi_1) + b_2 \sin(\omega_2 t + \phi_2) + \ldots + b_n \sin(\omega_n t + \phi_n) \quad (13)$$

where $\phi_1, \phi_2, \ldots, \phi_n$ are the phase offsets for each harmonic function.

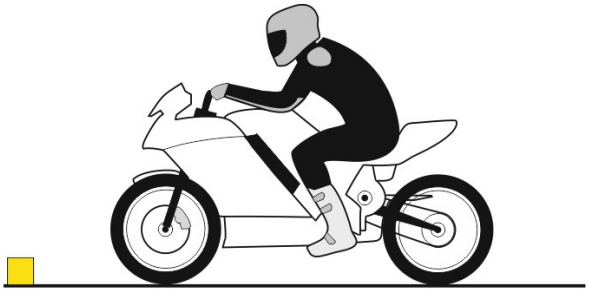

FIGURE 4: EXPERIMENTAL DESIGN FOR RIDE TEST , EQN. (??): $z = (r, \phi)$ [3]

5. EXPERIMENTAL DESIGN

The SV 106D multi-channel (6-channel) vibration analyzer meets the requirements of ISO 8041-1:2017 and complies with measurements according to ISO 2631-1,2 and 5, ISO 5349, and Directive 2002/44/EC. SV 106D allows simultaneous measurements with two triaxial accelerometers. SV 106D can simultaneously perform 1/1 or 1/3 octave real-time analysis with meter mode [6]. Svantek 106D is positioned on the seat of passenger, output $y = x_3(t)$. AX6 6-Axis accelerometers are positioned on the front, input $x_1(t)$, and rear suspensions, input $x_2(t)$. The experimental investigations have analyzed the conditions of comfort on the roads with artificial bumps. The stretches of road that precede and follow the artificial bumps present the statistical length and amplitude for road irregularity proposed in Table 1. The speed of the motorbike is about 50 km/h (Fig.4).

6. RESULTS

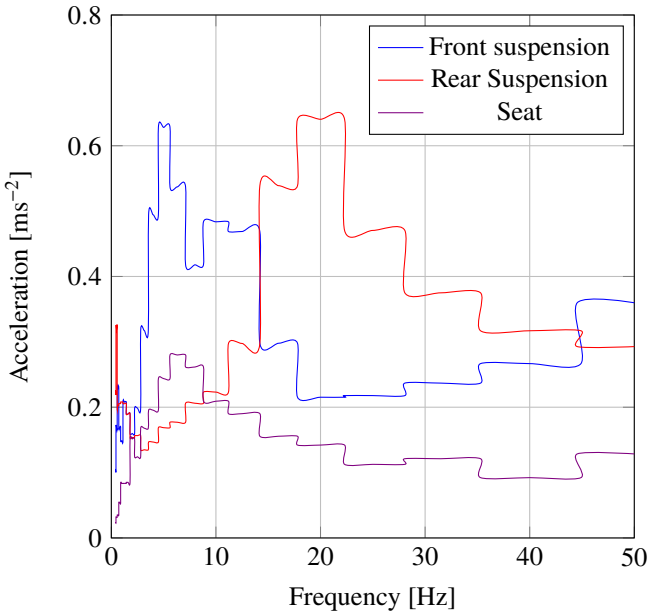

FIGURE 5: ACCELERATION DATA ACQUIRED ON THE FRONT AND REAR SUSPENSIONS, ON THE SEAT OF PASSENGER DURING RIDE TEST, EQN. (4) [3]

Figure 5 shows acceleration data acquired on the front and rear suspensions, on the seat of passenger during ride test in time domain. Figure 6 shows the evaluated frequency response functions $H_1(f)$ and $H_2(f)$ by the proposed MIMO process in frequency domain. The poles of the evaluated frequency response functions $H_1(f)$ and $H_2(f)$ describe two different map in the Figure 7. The comparison in the Figure 8 illustrates that $H_1(f)$ zeros describe a small area relative to the extent represented by $H_2(f)$ zeros. The damping ratio of the frequency response function $H_1(f)$ indicates the range 0.121-1. The damping ratio of the frequency response function $H_2(f)$ shows the range 0.05-0.26 (Fig.9). The Fig.**??** shows the comparison between accelerations obtained by MIMO process and ones deduced by experimental investigations on the seat of passenger.

7. DISCUSSION

The modal identification shall propose the assessment of the performance of the motorbike. The frequency responses derived through the proposed MIMO process highlight the motorbike's performance during the riding test. The application of the theorem of partial fraction expansion shows an excellent convergence between the acceleration, deduced with the frequency responses, and that acquired in the experimental investigation on the passenger seat. The accelerations acquired on the motorbike's front, and rear shock absorber assume the same maximum values, respectively, at 5 Hz and 20 Hz. Frequency response $H_1(f)$ has low acceleration values in the range 0.4-1.6 Hz; assumes high values 2-12.5 Hz; decreases in the range 16-31.5 Hz. Frequency response $H_2(f)$ accepts high acceleration values in the field 0.4-1 Hz. The areas described by the poles, zeros, and damping ratio

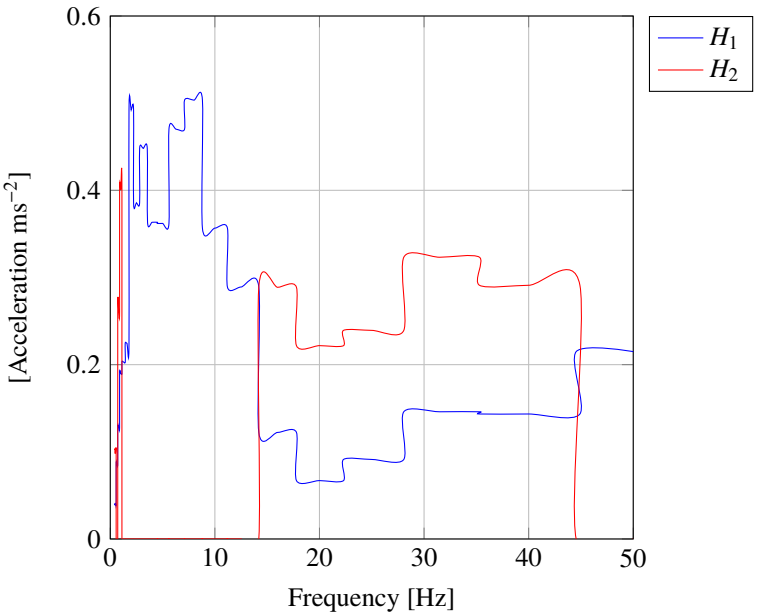

FIGURE 6: FREQUENCY RESPONSE FUNCTIONS, EQN. (4) [3]

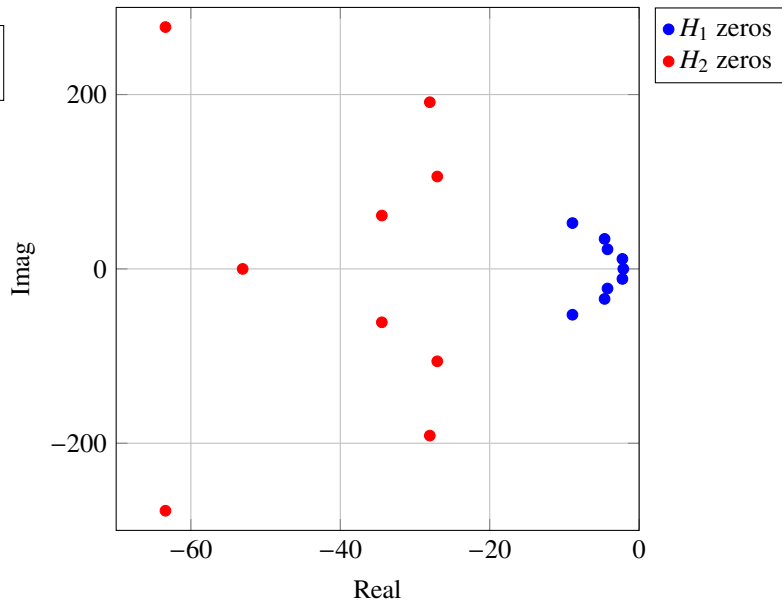

FIGURE 8: ZEROS OF FREQUENCY RESPONSE FUNCTIONS, EQN. (4) [3]

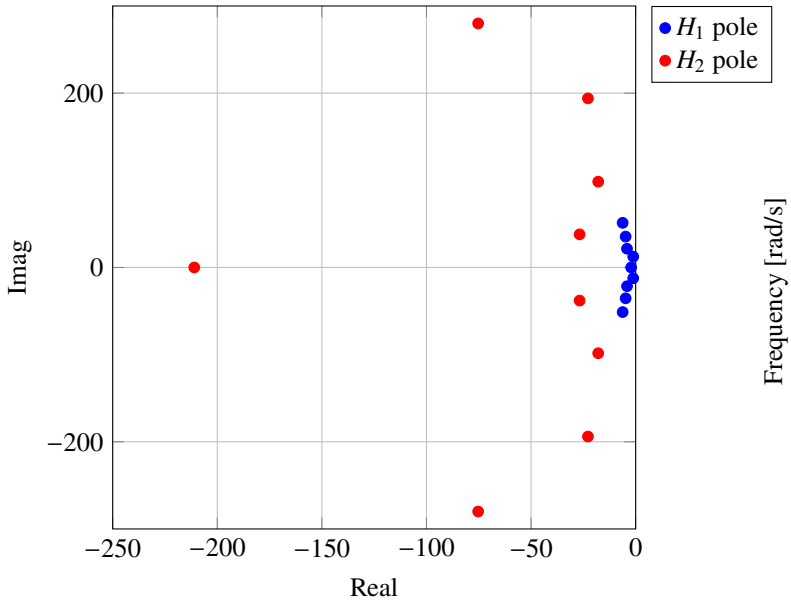

FIGURE 7: POLES OF FREQUENCY RESPONSE FUNCTIONS, EQN. (4) [3]

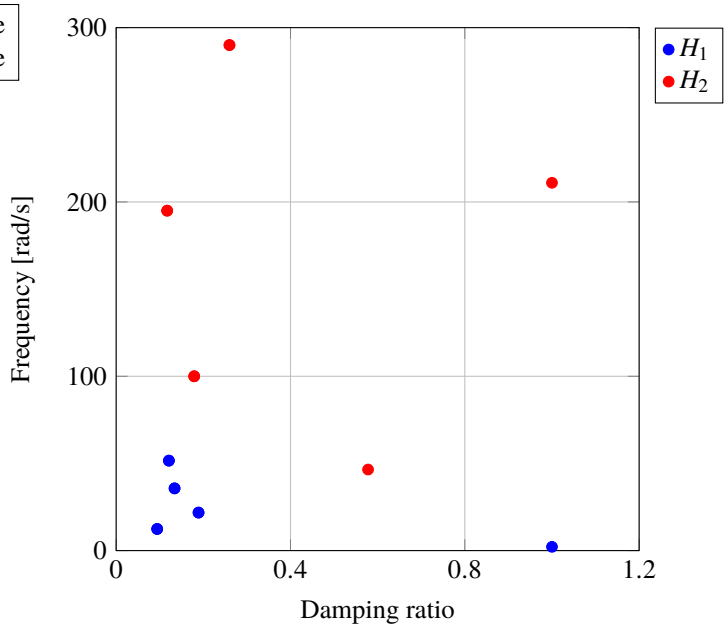

FIGURE 9: DAMPING RATIO VS. FREQUENCY, EQN. (4) [3]

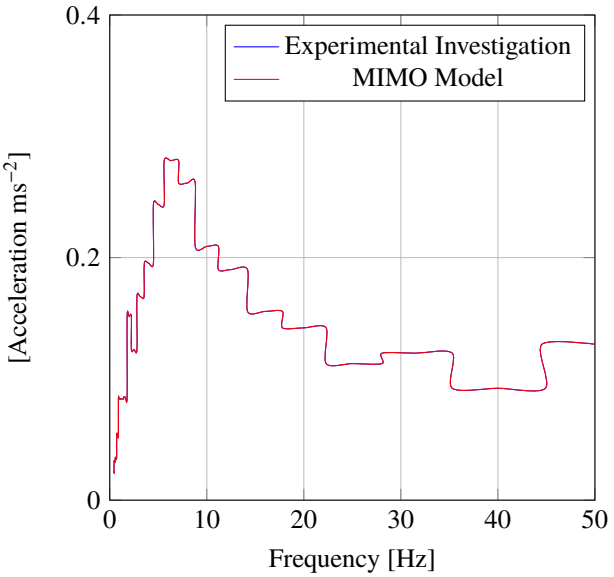

FIGURE 10: COMPARISON BETWEEN ACCELERATIONS OBTAINED BY MIMO PROCESS AND ONES DEDUCED BY EXPERIMENTAL INVESTIGATIONS ON THE SEAT OF PASSENGER, EQN. (4) [3]

values of the $H_1(f)$ frequency response are smaller than those of the poles, zeros, and damping ratio values of the $H_2(f)$ frequency response. The front and rear shock absorbers perform complementary actions to ensure the motorbike's comfort.

8. CONCLUSION

A MIMO process has been developed to characterize the dynamic response of the motorbike excited by road profiles by modal properties of the motorbike. The MIMO process is calibrated by the ride test. The least square error evaluates the good agreement between accelerations obtained by MIMO process and ones deduced by experimental investigations on the seat of passenger.

ACKNOWLEDGMENTS

The research described in this paper was supported by the grants from the Research Grants FAR 2022.

REFERENCES

[1] Cossalter V., Da Lio M.,Lot R., Fabbri L., A General Method for the Evaluation of Vehicle Manoeuvrability with Special Emphasis on Motorcycles, Vehicle System Dynamics, 31, 2, 1999, pp.113–135, 10.1076/vesd.31.2.113.2094.

[2] Figliolini, G., Lanni, C., and Angeles, J. (April 13, 2020). "Kinematic Analysis of the Planar Motion of Vehicles when Traveling Along Tractrix Curves." ASME. J. Mechanisms Robotics. October 2020; 12(5): 054502. https://doi.org/10.1115/1.4046509

[3] Cavacece, M., Figliolini, G., Lanni, C., "Vertical Vibrations of the Vehicle Excited by Ride Test". In: Rao, Y.V.D., Amarnath, C., Regalla, S.P., Javed, A., Singh, K.K. (eds) Advances in Industrial Machines and Mechanisms. Lec- ture Notes in Mechanical Engineering. Springer, Singapore, 2021, https://doi.org/10.1007/978-981-16-1769-057.

[4] Cavacece,M.,"ComfortAssessmentinRailwayVehiclesby an Optimal Identification of Transfer Function," Universal Journal of Mechanical Engineering, Vol. 10, No. 1, pp. 1–12, 2022. DOI: 10.13189/ujme.2022.100101.

[5] Cavacece, M., "Incidence of Predisposing Factors on the Human Hand-arm Response with Flexed and Extended Elbow Positions of Workers Subject to Different Sources of Vibrations," Universal Journal of Public Health, Vol. 9, No. 6, pp. 507 - 519, 2021. DOI: 10.13189/ujph.2021.090620.

[6] ISO, Mechanical vibration and shock: Evaluation of human exposure to whole-body vibration. International Standard, ISO 2631-1:2014, 2014.